The Journal of Veterinary Medical Science

NOTE

Internal Medicine

Histopathological and aquaporin7 mRNA expression analyzes in the skeletal and cardiac muscles of obese *db/db* mice

Yoshihiro WAKAYAMA[1,2)]*, Satoshi HIRAKO[3)], Hirokazu OHTAKI[2)], Satoru ARATA[4-6)], Takahiro JIMI[7)] and Kazuho HONDA[2)]

[1)]Wakayama Clinic, 2-3-18 Kanai, Machida-shi, Tokyo 195-0072, Japan
[2)]Department of Anatomy, Showa University School of Medicine, 1-5-8 Hatanodai, Shinagawa-ku, Tokyo 142-8555, Japan
[3)]Department of Health and Nutrition, University of Human Arts and Sciences, 1288 Magome, Iwatsuki-shi, Saitama 339-8539, Japan
[4)]Center for Biotechnology, Showa University, 1-5-8 Hatanodai, Shinagawa-ku, Tokyo 142-8555, Japan
[5)]Center for Laboratory Animal Science, Showa University, 1-5-8 Hatanodai, Shinagawa-ku, Tokyo 142-8555, Japan
[6)]Department of Biochemistry, Faculty of Arts and Sciences, Showa University, 4562 Kamiyoshida, Fujiyoshida-shi, Yamanashi 403-0005, Japan
[7)]Division of Neurology, Machida Keisen Hospital, 2-1-47 Minamimachida, Machida-shi, Tokyo 194-005, Japan

J. Vet. Med. Sci.
83(7): 1155–1160, 2021
doi: 10.1292/jvms.20-0470

Received: 20 August 2020
Accepted: 16 May 2021
Advanced Epub:
31 May 2021

ABSTRACT. The aim of this study is to examine 1) muscle fiber type composition, 2) myofiber diameter, and 3) aquaporin (AQP) 7 and AQP 9 mRNA expressions by quantitative PCR in muscles of obese *db/db* mice. The myofiber type composition of skeletal muscle was not statistically significantly different between *db/db* mice and control mice; while the average myofiber diameter ratio showed a decrease in *db/db* mice. The expression of AQP7 but not AQP9 mRNA in the skeletal and cardiac muscles was significantly upregulated in *db/db* mice. Thus this study revealed quantitatively that type 2 myofiber atrophy was shown in the skeletal muscles of *db/db* mice. AQP7 mRNA expression was upregulated in the skeletal and cardiac muscles of *db/db* mice.

KEY WORDS: aquaporin 7 mRNA, cardiac muscle, *db/db* mouse, quantitative polymerase chain reaction, skeletal

Skeletal muscle is composed of about 42 percent of the average human body mass and the total muscle mass including cardiac and smooth muscles are about 45 percent in total [24]. The next most abundant tissue, the adipose tissue, is normally composed of about 18 percent of the total body mass [24]. So glucose and lipid metabolism in skeletal muscle cells is very important in the energy production [24]. Obesity significantly reduces metabolism in skeletal muscle cells, inducing a state of insulin resistance [26].

Insulin resistance accelerates muscle protein degradation by activation of the muscle cell ubiquitin-proteasome pathway and this is a defect of intracellular signaling in muscle cells [29, 37]. These phenomena lead to an atrophy of skeletal muscles and the dysfunction of muscle cells [37].

The impairment of skeletal muscle function is caused by many diseases of skeletal muscles such as muscular dystrophies, polymyositis, dermatomyositis, neurogenic amyotrophy and so on. However, knowledge of the muscle pathology in the obese animals is relatively limited.

With regard to myopathology of obese animals, several groups of investigators reported that the insulin resistance and obesity are associated with the relative increases in the proportion of glycolytic fast twitch type 2 myofibers and decreases in the proportion of oxidative slow twitch type 1 myofibers [1, 10, 17, 18]. Among these investigators, two groups showed the increased proportion of type 2b myofibers [10, 18], whereas, another group showed an increase of type 2a myofibers [17]. Kempen *et al*. [15] reported no change in myofiber type proportion in obese women. On the other hand, Warmington *et al*. [38] showed that myofiber type proportions display a slower type profile in the obese *ob/ob* skeletal muscle. Therefore, with regard to the myopathology of the obese skeletal muscle, consistent myopathological findings have not yet been determined so far.

Myofiber types are usually determined by the use of histochemistry, however, the HE stained muscle samples of cryosections of non-fixed frozen muscle are also available for this aim [7]. Thus, in this study, by using HE stained non-fixed muscle sections, the

*Correspondence to: Wakayama, Y.: wakayama@med.showa-u.ac.jp

histopathology of skeletal muscles in leptin-receptor mutated obese *db/db* mice was investigated.

An increase in lipid content has been reported in the skeletal muscle cells of obese animals [14, 23, 28, 32, 33]. The increased lipid content, such as triglycerides, in the skeletal and / or cardiac muscle cells is synthesized with glycerol and fatty acids in the muscle cells. Aquaporin (AQP) 7 and AQP9 are aquaglyceroporins present in the muscle cell plasma membrane and transport the glycerol as well as water molecules [2, 11, 34]. Among these aquaporins, AQP7 is now implicated as a central agent in controlling fat metabolism [9]. An initial hypothesis was therefore that the expression of AQP7 and AQP9 at the muscle cell membrane may be upregulated in the obese *db/db* mice. To test this hypothesis, the expression of AQP7 and AQP9 mRNAs was measured using quantitative PCR in the skeletal and cardiac muscles of obese *db/db* and lean control mice.

Male leptin receptor mutant (*db/db*) mice on a C57BL/6 background, along with wild type C57BL/6 mice were obtained from Sankyo Laboratory Service Corp. (Tokyo, Japan). To avoid potential gender-specific differences, male mice only were used because of the relatively homogeneous metabolic phenotype of males compared with that of females in the *db/db* mice. The *db/db* mice and wildtype C57BL/6 mice were fed with standard chow diet (PMI LabDiet #5058, St. Louis, MO, USA) starting at 7 weeks of age and continuing for 12 weeks. Eight obese *db/db* mice and 8 ages matched lean wild mice at five months of age were sacrificed by cervical dislocation and the quadriceps femoris and cardiac muscles were excised from each mouse. Immediately after excision, the muscle samples were frozen in isopentane cooled with liquid nitrogen. Among these samples, the skeletal muscles of 4 *db/db* and 4 lean control mice were cut into 6-µm thick cross sections by using cryostat. Further, the skeletal and cardiac muscles from 8 *db/db* and 8 lean mice were processed for quantitative real time RT-PCR analysis.

Experimental protocols were approved and followed by the Institutional Animal Care and Use Committee of Showa University (Permit Number: 57022, 58016 and 59017), which operates in accordance with the Japanese Government for the care and use of laboratory animals.

Frozen 6 µm thick cross-sections of the skeletal muscles were placed on slide glasses and stained with hematoxylin and eosin (HE). The HE stained muscle samples were examined and photographed at random by Nikon H550L microscope. The fiber type composition was examined at least in 100 myofibers in each mouse and was expressed as a ratio of type 1 fiber number versus type 2 fiber number (type 2 / type 1) in each mouse. Furthermore, the myofiber diameter and myofiber diameter ratio of type 1 versus type 2 (type 2 / type 1) was calculated by comparing total diameters of 50 type 1 and 50 type 2 myofibers, respectively, in each mouse. Analyses were done in the photographs enlarged to × 500. In the measurement of myofiber diameter, the shortest diameter of each myofiber was measured in this study. The photographs both from 4 *db/db* mice and 4 control lean mice were coded and mixed, and were analyzed using a single blind method. After finishing all analyses, the photographs were decoded and statistically compared in two groups.

The HE stained cross-sections of the frozen quadriceps femoris muscle samples of normal control mouse showed the slight variation of myofiber diameter. The myofibers with a greater diameter usually have slightly lighter myocellular sarcoplasmic coloring (type 2 fibers) (Fig. 1A). Dubowitz and Brooke [7] described that the type 1 fibers are usually characterized by slightly darker background coloring (Fig. 1A). On the other hand, the HE stained quadriceps femoris muscle sections of obese *db/db* mouse revealed a more marked variation of myofiber diameter (Fig. 1B) than that seen in the control lean mouse (Fig. 1A). The myofibers with brighter myocellular sarcoplasmic coloring displayed a more pronounced variation of myofiber size (Fig. 1B). Furthermore both fiber types in Fig. 1B seem to have either a) invaginations of the plasma membrane or b) internal vacuoles or c) lipid droplets. With regard to the myofiber type composition of the obese *db/db* mouse, it appeared to be similar to that seen in the control lean mouse (Fig. 1A, 1B).

Throughout this study including the histopathological analysis of this study, data were presented as group mean ± standard error of the mean (S.E.). The difference between *db/db* mouse group and wild mouse group was evaluated using two-tailed *t*-test. A *P*-value less than 0.05 was considered to be statistically significant.

The myofiber type composition with regard to the type 2 versus type 1 myofibers, the group mean ratio ± S.E. was 1.97 ± 0.21 in the *db/db* mouse group and was 2.21 ± 0.25 in the control lean mouse group, respectively. The differences between these values were not statistically significant (P=0.494) (Table 1).

With regard to the type 1 myofiber diameter (µm), the group mean ± S.E. was 19.1 ± 0.3 in the *db/db* mouse group and was 23.3 ± 2.5 in the control lean mouse group, respectively (P=0.141); while in type 2 myofiber diameter (µm), it was 28.2 ± 0.9 in the *db/db* mouse group and 40.4 ± 3.6 in the control mouse group, respectively (P=0.016) (Table 2).

The myofiber diameter ratio with regard to the type 2 versus type 1 myofibers, the group mean ratio ± S.E. was 1.48 ± 0.03 in the *db/db* mouse group and was 1.75 ± 0.09 in the control lean mouse group, respectively. The smaller type 2 fiber diameter in *db/db* mouse group was shown in this study (P=0.034) (Table 3).

Total RNA was extracted from each muscle sample of 8 obese *db/db* mice and 8 lean wild mice using TRIzol (Invitrogen, Carlsbad, CA, USA). Concentrations of mouse AQP7and AQP9 mRNAs contents were estimated by quantitative PCR (QPCR). First-strand cDNA was synthesized using AffinityScript QPCR cDNA Synthesis Kit (Agilent Technologies, Santa Clara, CA, USA) and 100 ng of extracted total RNA. Oligonucleotide primer sets were designed from mouse AQP7 [Mus musculus AQP7, MA101958, TaKaRa, Kusatsu, Japan], mouse AQP9 [Mus musculus AQP9, MA117402, TaKaRa], sequences: mouse AQP7 mRNA: sense strand, 5′-TGGGTTTTGGATTCGGAGT-3′; antisense strand, 5′-TGTTCTTCTTGTCGGTGATGG-3′; and the mouse AQP9 mRNA: sense strand, 5′-CTCAACTCTGGTTGTGCCATGAA-3′; antisense strand, 5′-ATCATAGGGCCCACGACAGGTA-3′. To compensate for differences in RNA quality or RT efficacy, expression of mouse glyceraldehyde 3-phosphate dehydrogenase (GAPDH) mRNA was measured in each muscle sample, although the election of the endogenous control genes in obese and diabetic models is not easy [6]. Oligonucleotide primers for GAPDH mRNA were designed as follows: sense strand,

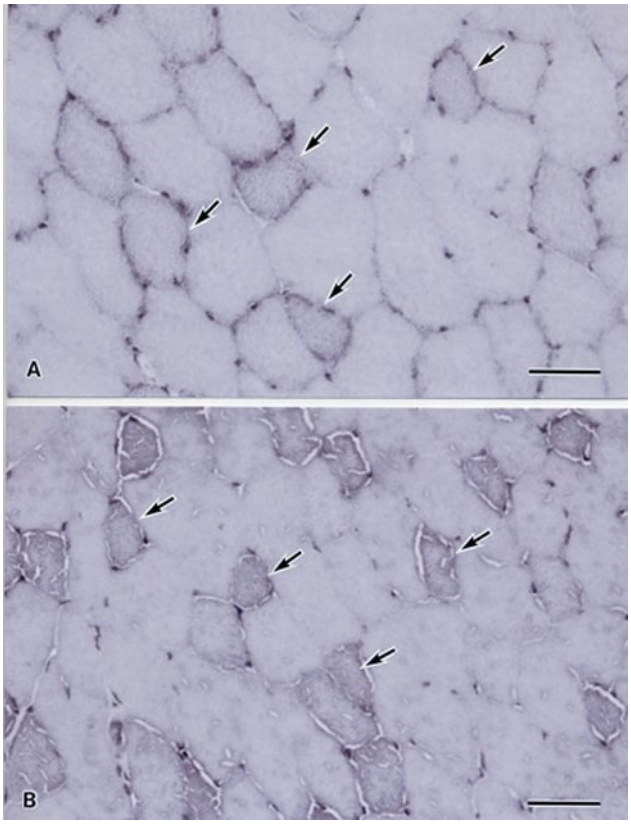

Fig. 1. Hematoxylin and eosin (HE) staining of the quadriceps femoris muscle of lean wild mouse (A) and obese *db/db* mouse (B). In wild mouse muscle (A), the scattered myofibers (arrows) with slightly darker sarcoplasmic appearance which correspond to type 1 myofibers are seen. In the *db/db* muscle (B), frequent occurrence of myofibers (arrows) with slightly darker sarcoplasmic background and numerous myofibers with brighter sarcoplasmic appearance are noted. The myofibers with slightly brighter sarcoplasmic appearance show the slightly smaller diameter. Furthermore both fiber types in Fig. 1B seem to have either a) invaginations of the plasma membrane or b) internal vacuoles or c) lipid droplets. Bar in A and B=50 µm.

5′-TGTGTCCGTCGTGGATCTGA-3′; antisense strand, 5′-CCTGCTTCACCACCTTCTTGAT-3′.

Each primer set for the measurement of mouse AQP7, mouse AQP9 and mouse GAPDH mRNA levels was mixed with the respective cDNA using SYBR Prime Script RT-PCR Kit II (TaKaRa). Real-time PCR was performed on an ABI Prism 7900 sequence detection system (Applied Biosystems, Foster, CA, USA) with thermocycler conditions including initial denaturation at 95°C for 30 sec followed by 45 cycles at 95°C for 5 sec, 60°C for 1 min with dissociative reaction of PCR products from 65°C to 95°C. Threshold cycle was calculated using the Sequence Detector Systems version (Applied Biosystems) by determining the cycle number. Mouse AQP7 and AQP9 mRNAs expressions were calculated using the standard curve method normalizing with that of mouse GAPDH mRNA internal control. Total RNAs from muscle samples of 8 *db/db* mice and 8 wild mice were analyzed in duplicate by using this method and the mean was calculated in each muscle sample.

The standard curve method was used for gene expression analysis. Two-fold dilutions of a reverse transcription product (cDNA) from a control group are used to construct a standard curve. The units could be the dilution values 1, 0.5, 0.25 and 0.125. The standard curves for the quantification of mouse AQP7 and AQP9 mRNAs was linear across 4 to 5 log ranges of RNA concentration. Correlation coefficients were 0.9852 and 0.9345 for mouse skeletal and cardiac muscle AQP7 mRNA, 0.9277 and 0.9345 for mouse skeletal and cardiac muscle AQP9 mRNA, respectively, and 0.9993 and 0.9853 for mouse skeletal and cardiac muscle GAPDH mRNA, respectively. Group mean ratios ± S.E. of mouse AQP7 mRNA copy number versus GAPDH mRNA copy number were 320.3 ± 72.0 and 100.0 ± 23.5 in the skeletal muscles of 8 obese *db/db* mice and 8 lean wild mice, respectively. These two ratios were statistically significantly different (P=0.011 two tailed t-test) (Table 4). The group mean rations ± S.E. of mouse AQP9 mRNA copy number versus GAPDH mRNA copy number were 111.2 ± 27.8 and 100.0 ± 16.2 in the skeletal muscles of 8 obese *db/db* mice and 8 lean wild mice, respectively. These two ratios were statistically non significant (P=0.734 two tailed t-test) (Table 5). On the contrary, the

Table 1. Myofiber type composition in obese *db/db* mice and lean control mice

	Myofiber type ratio (type 2/type 1) Group mean ± S.E.	*P*
db/db mouse group (n=4)	1.97 ± 0.21	0.494*
Control mouse group (n=4)	2.21 ± 0.25	

*P=0.494 by two tailed t test. S.E.: standard error.

Table 2. Myofiber diameter in obese *db/db* mice and lean control mice

	Type 1 fiber diameter Group mean ± S.E. (µm)	*P*	Type 2 fiber diameter Group mean ± S.E. (µm)	*P*
db/db mouse group (n=4)	19.1 ± 0.3	0.141*	28.2 ± 0.9	0.016**
Control mouse group (n=4)	23.3 ± 2.5		40.4 ± 3.6	

*P=0.141 by two tailed t test. **P=0.016 by two tailed t test. S.E.: standard error.

Table 3. Myofiber diameter ratio in obese *db/db* mice and lean control mice

	Myofiber diameter ratio (type 2/type 1) Group mean ± S.E.	*P*
db/db mouse group (n=4)	1.48 ± 0.03	0.034*
Control mouse group (n=4)	1.75 ± 0.09	

*P=0.034 by two tailed t-test. S.E.: standard error.

Table 4. Expression of aquaporin (AQP) 7 mRNA in the skeletal and cardiac muscles of the obese *db/db* mice and lean control mice

	AQP7 mRNA expression ratio (AQP7/GAPDH)#			
	Skeletal muscle	*P*	Cardiac muscle	*P*
db/db mouse group (n=8)	320.3 ± 72.0*	0.011	214.1 ± 44.8*	0.047
Control mouse group (n=8)	100.0 ± 23.5		100.0 ± 27.2	

*Group mean ± standard error of the mean. P values were calculated by two-tailed t test. #Mouse AQP7 mRNA copy number / mouse glyceraldehyde 3-phosphate dehydrogenase (GAPDH) mRNA copy number.

Table 5. Expression of aquaporin (AQP) 9 mRNA in the skeletal and cardiac muscles of the obese *db/db* mice and lean control mice

	AQP9 mRNA expression ratio (AQP9/GAPDH)#			
	Skeletal muscle	*P*	Cardiac muscle	*P*
db/db mouse garoup (n=8)	111.2 ± 27.8*	0.734	80.6 ± 14.5*	0.454
Control mouse group (n=8)	100.0 ± 16.2		100.0 ± 20.6	

*Group mean ± standard error. P values were calculated by two-tailed t-test. #Mouse AQP9 mRNA copy number / mouse glyceraldehyde 3-phosphate dehydrogenase (GAPDH) mRNA copy number.

Table 6. CT values of glyceraldehyde 3-phosphate dehydrogenase for obese *db/db* mice and lean control mice

	Skeletal muscle	*P*	Cardiac muscle	*P*
db/db mouse group (n=8)	16.02 ± 0.14*	0.616	16.60 ± 0.34*	0.905
Control mouse group (n=8)	16.23 ± 0.37		16.55 ± 0.32	

*Group mean ± standard error. P values were calculated by two-tailed t test.

group mean ratios ± S.E. of mouse cardiac muscle AQP7 mRNA copy number versus GAPDH mRNA copy number in the 8 obese *db/db* mice and 8 lean wild mice were 214.1 ± 44.8 and 100.0 ± 27.2, respectively. The differences of these ratios were also statistically significant (P=0.047 two tailed t test) (Table 4). The group mean ratios ± S.E. of mouse cardiac muscle AQP9 mRNA copy number versus GAPDH mRNA copy number were 80.6 ± 14.5 and 100.0 ± 20.6 in the 8 obese *db/db* mice and 8 lean control mice, respectively. The differences of these two ratios were statistically non significant (P=0.454 two tailed t test) (Table 5). The group mean ± S.E. for the Ct values of GAPDH of the skeletal and cardiac muscles for the *db/db* mouse group and control mouse group was shown in Table 6.

Obesity is one of the metabolic syndrome and relates to the high incidence of the life threatening diseases such as diabetes mellitus, cerebrovascular disease and / or myocardial infarction. The skeletal muscle is the major site of metabolism in the body. Many papers have so far reported the myopathology of the obese animals, some of which were listed in the references of this paper [1, 10, 15, 17, 18] and these papers described that the skeletal muscles of obese animals showed the decreased cross-sectional areas qualitatively without measuring the myofiber diameter. We studied the myopathology of obese *db/db* mice qualitatively and quantitatively. Our results revealed that type 2 myofiber diameter was smaller in *db/db* mice than that in the lean control mice and this finding was confirmed statistically. This means that the muscle of *db/db* mouse is atrophic especially in fast twitch type 2 white myofibers. However, the myofiber type proportion was not statistically different between the obese *db/db* mice and lean control mice, although the ratio of type 2 to type 1 was relatively low in *db/db* mice. Furthermore both fiber types in *db/db* mice seemed to have either a) invaginations of the plasma membrane or b) internal vacuoles or c) lipid droplets. Electron microcopy will provide us more information about this problem. The type 2 fiber atrophy of the obese *db/db* mice seen in this study may result partly from the immobility of the obese *db/db* mice. Kemp *et al*. [14] also analyzed morphologically the sternomastoid (first twitch type 2 fiber), extensor digitorum longus (fast twitch type 2 fiber) and soleus (slow twitch type 1 and fast twitch type 2 mixed) muscles of leptin deficient obese *ob/ob* mice and lean control mice, and found that all three muscles were smaller in size with the type 2

atrophy mass being the most affected in comparison with muscles of lean control mice. Such type 2 myofiber atrophy may derive from the lower activity level of the animal (functional disuse) [28] in addition to hormonal (such as elevated glucocorticoids and adipokines) and other physical changes [14, 27] in the obese mice. In addition, the findings of reduced activity of the mitochondrial fatty acid oxidation (mFAO) pathway *in vitro*, lower abundance of ACAD9 and CPT1B, and decreased acylcarnitines *in vivo* firmly support that the mFAO pathway in the skeletal muscle of diabetic mice is attenuated, possibly resulting in cell/tissue dysfunction in diabetes [41]. The impairment of muscle regeneration may also increase in pathological conditions such as muscle atrophy of obese mice [23, 40]. The muscle satellite cell is a dormant myoblast [22] and is reported to increase in pathological conditions such as muscular dystrophy [31, 36]. The altered proliferation and differentiation of satellite cells were also described in obese mice [3, 25]. Taken together, this event is also linked to the muscle atrophy in the obese mice. Furthermore, metabolic defects such as insulin resistance accelerates muscle protein degradation by activating the ubiquitin-proteasome pathway and defective muscle cell signaling, leads to muscle atrophy in obese animals [29, 37].

With regard to the myofiber type proportion in the quadriceps femoris muscles, the result of our study revealed no difference between obese *db/db* mouse muscle and lean control mouse muscle. As described previously some groups of investigators reported the increased proportion of fast twitch glycolytic type 2 muscle fibers in the obese animals [10, 17, 18]; while other investigators reported that fiber proportions of obese mice displayed higher numbers of slow twitch type 1 profile muscle fibers [38]. So a definite conclusion about the fiber type proportion in the skeletal muscle of obese animal has not so far been reached. Skeletal muscle is composed of heterogeneous muscle fibers which differ in their metabolic and contractile profile and are called type 1 and type 2 fibers [30]. Type 1 fibers have an enhanced capacity for mitochondrial respiration and fatty acid oxidation and contain slow isoforms of contractile proteins (slow myosin); whereas type 2 fibers preferentially oxidise glucose and contain fast twitch contractile proteins (fast myosin) [30]. Intramyofiber lipid droplets are increased in the skeletal muscle cells of obese animal [5, 32, 33, 39]. The fatty acids derived from the intramyocellular lipid droplets are metabolized in the mitochondria by β-oxidation. The number of mitochondria is greater in type 1 myofibers, so the increased proportion of type 1 fibers in the obese skeletal muscles would be reasonable. From this perspective, the reported mechanism concerning an increased proportion of type 2 myofibers in obese animals is unclear. Further investigations are necessary in order to solve this problem.

AQPs are the small intrinsic channel-forming membrane proteins of epithelial and endothelial cells, and are classified into two groups [2]. One group of AQPs functions as a water-selective transport channel and another group contains AQPs with a water channel permeable to neutrally charged small molecules such as glycerol, urea and purines [2, 12, 13, 16]. The latter AQPs are called aquaglyceroporins in which AQP3, AQP7, AQP9 and AQP10 are included [2, 21]. With regard to lipid metabolism, glycerol is an important molecule and direct source of glycerol 3 phosphate to synthesize triglyceride [4], which is a main substance of neutral lipid. AQP7 and AQP9 are considered to be a gateway for the influx and efflux of circulating and /or lipolysis-derived glycerol from adipocytes and/or hepatocytes [8, 16, 20]. In this study, it was hypothesized that AQP7 and AQP9 mRNAs expression would be altered in the obese *db/db* mouse skeletal and cardiac muscles, since the neutral lipid, in which the triglyceride was a main substance, was increasing in these cells. As was observed in the skeletal muscles of obese *ob/ob* mice [33] and in diet induced obesity mice [32], upregulation of AQP7, but not AQP9 mRNAs in skeletal and cardiac muscles of *db/db* mice was revealed in this study. Increased AQP7 abundance was also described in skeletal muscle from obese men with type 2 diabetes [19]. These findings were thought to be reasonable, since AQP7 is a channel for glycerol molecules in skeletal and cardiac muscle cell membranes, and increased extracellular glycerol might enter myocytes through an increased number of AQP7 glycerol channels possibly associated with an increase in AQP7 mRNA expression. It would be interesting to see whether the obese *db/db* muscles show altered expression of other AQPs such as AQP4, as was observed in the skeletal muscle with Duchenne muscular dystrophy [35], since AQP7 is not only glycerol channel but also water channel.

Finally, the present study shed some light on the pathophysiology of lipid metabolism in the muscles of obese *db/db* mice.

POTENTIAL CONFLICTS OF INTEREST. The authors have nothing to disclose.

ACKNOWLEDGMENT. We would like to thank Ms. H. Ozawa for her assistance with manuscript preparation.

REFERENCES

1. Acevedo, L. M., Raya, A. I., Ríos, R., Aguilera-Tejero, E. and Rivero, J. L. 2017. Obesity-induced discrepancy between contractile and metabolic phenotypes in slow- and fast-twitch skeletal muscles of female obese Zucker rats. *J Appl Physiol (1985)* **123**: 249–259. [Medline] [CrossRef]
2. Agre, P. 2004. Nobel Lecture. Aquaporin water channels. *Biosci. Rep.* **24**: 127–163. [Medline] [CrossRef]
3. Arounleut, P., Bowser, M., Upadhyay, S., Shi, X. M., Fulzele, S., Johnson, M. H., Stranahan, A. M., Hill, W. D., Isales, C. M. and Hamrick, M. W. 2013. Absence of functional leptin receptor isoforms in the POUND (Lepr(db/lb)) mouse is associated with muscle atrophy and altered myoblast proliferation and differentiation. *PLoS One* **8**: e72330. [Medline] [CrossRef]
4. Baba, H., Zhang, X. J. and Wolfe, R. R. 1995. Glycerol gluconeogenesis in fasting humans. *Nutrition* **11**: 149–153. [Medline]
5. Baek, K. W., Cha, H. J., Ock, M. S., Kim, H. S., Gim, J. A. and Park, J. J. 2018. Effects of regular-moderate exercise on high-fat diet-induced intramyocellular lipid accumulation in the soleus muscle of Sprague-Dawley rats. *J. Exerc. Rehabil.* **14**: 32–38. [Medline] [CrossRef]
6. Catalán, V., Gómez-Ambrosi, J., Rotellar, F., Silva, C., Rodríguez, A., Salvador, J., Gil, M. J., Cienfuegos, J. A. and Frühbeck, G. 2007. Validation of endogenous control genes in human adipose tissue: relevance to obesity and obesity-associated type 2 diabetes mellitus. *Horm. Metab. Res.* **39**: 495–500. [Medline] [CrossRef]
7. Dubowitz, V. and Brooke, M. H. 1973. Histological and histochemical stains and reactions. pp. 20–33. In: Muscle Biopsy: A Modern Approach

(Dobowitz V. and Brooke M. H. eds.), W.B. Saunders Co., Philadelphia.
8. Frühbeck, G. 2001. A heliocentric view of leptin. *Proc. Nutr. Soc.* **60**: 301–318. [Medline] [CrossRef]
9. Frühbeck, G. 2005. Obesity: aquaporin enters the picture. *Nature* **438**: 436–437. [Medline] [CrossRef]
10. Holmäng, A., Brzezinska, Z. and Björntorp, P. 1993. Effects of hyperinsulinemia on muscle fiber composition and capitalization in rats. *Diabetes* **42**: 1073–1081. [Medline] [CrossRef]
11. Inoue, M., Wakayama, Y., Kojima, H., Shibuya, S., Jimi, T., Hara, H., Iijima, S., Masaki, H., Oniki, H. and Matsuzaki, Y. 2009. Aquaporin 9 expression and its localization in normal skeletal myofiber. *J. Mol. Histol.* **40**: 165–170. [Medline] [CrossRef]
12. Ishibashi, K., Kuwahara, M., Gu, Y., Kageyama, Y., Tohsaka, A., Suzuki, F., Marumo, F. and Sasaki, S. 1997. Cloning and functional expression of a new water channel abundantly expressed in the testis permeable to water, glycerol, and urea. *J. Biol. Chem.* **272**: 20782–20786. [Medline] [CrossRef]
13. Ishibashi, K., Kuwahara, M., Gu, Y., Tanaka, Y., Marumo, F. and Sasaki, S. 1998. Cloning and functional expression of a new aquaporin (AQP9) abundantly expressed in the peripheral leukocytes permeable to water and urea, but not to glycerol. *Biochem. Biophys. Res. Commun.* **244**: 268–274. [Medline] [CrossRef]
14. Kemp, J. G., Blazev, R., Stephenson, D. G. and Stephenson, G. M. 2009. Morphological and biochemical alterations of skeletal muscles from the genetically obese (ob/ob) mouse. *Int. J. Obes.* **33**: 831–841. [Medline] [CrossRef]
15. Kempen, K. P., Saris, W. H., Kuipers, H., Glatz, J. F. and Van Der Vusse, G. J. 1998. Skeletal muscle metabolic characteristics before and after energy restriction in human obesity: fibre type, enzymatic beta-oxidative capacity and fatty acid-binding protein content. *Eur. J. Clin. Invest.* **28**: 1030–1037. [Medline] [CrossRef]
16. Kishida, K., Kuriyama, H., Funahashi, T., Shimomura, I., Kihara, S., Ouchi, N., Nishida, M., Nishizawa, H., Matsuda, M., Takahashi, M., Hotta, K., Nakamura, T., Yamashita, S., Tochino, Y. and Matsuzawa, Y. 2000. Aquaporin adipose, a putative glycerol channel in adipocytes. *J. Biol. Chem.* **275**: 20896–20902. [Medline] [CrossRef]
17. Klueber, K. M., Feczko, J. D., Schmidt, G. and Watkins, J. B. 3rd. 1989. Skeletal muscle in the diabetic mouse: histochemical and morphometric analysis. *Anat. Rec.* **225**: 41–45. [Medline] [CrossRef]
18. Kriketos, A. D., Pan, D. A., Lillioja, S., Cooney, G. J., Baur, L. A., Milner, M. R., Sutton, J. R., Jenkins, A. B., Bogardus, C. and Storlien, L. H. 1996. Interrelationships between muscle morphology, insulin action, and adiposity. *Am. J. Physiol.* **270**: R1332–R1339. [Medline]
19. Lebeck, J., Søndergaard, E. and Nielsen, S. 2018. Increased AQP7 abundance in skeletal muscle from obese men with type 2 diabetes. *Am. J. Physiol. Endocrinol. Metab.* **315**: E367–E373. [Medline] [CrossRef]
20. Margetic, S., Gazzola, C., Pegg, G. G. and Hill, R. A. 2002. Leptin: a review of its peripheral actions and interactions. *Int. J. Obes. Relat. Metab. Disord.* **26**: 1407–1433. [Medline] [CrossRef]
21. Matsuzaki, T., Hata, H., Ozawa, H. and Takata, K. 2009. Immunohistochemical localization of the aquaporins AQP1, AQP3, AQP4, and AQP5 in the mouse respiratory system. *Acta Histochem. Cytochem.* **42**: 159–169. [Medline] [CrossRef]
22. Mauro, A. 1961. Satellite cell of skeletal muscle fibers. *J. Biophys. Biochem. Cytol.* **9**: 493–495. [Medline] [CrossRef]
23. Nguyen, M. H., Cheng, M. and Koh, T. J. 2011. Impaired muscle regeneration in ob/ob and db/db mice. *ScientificWorldJournal* **11**: 1525–1535. [Medline] [CrossRef]
24. Ontko, J. A. 1986. Lipid metabolism in muscle. pp. 697–720. In: Myology (Engel, A. G. and Banker, B. Q. eds.), McGraw-Hill Inc., New York.
25. Purchas, R. W., Romsos, D. R., Allen, R. E. and Merkel, R. A. 1985. Muscle growth and satellite cell proliferative activity in obese (OB/OB) mice. *J. Anim. Sci.* **60**: 644–651. [Medline] [CrossRef]
26. Qiu, S., Mintz, J. D., Salet, C. D., Han, W., Giannis, A., Chen, F., Yu, Y., Su, Y., Fulton, D. J. and Stepp, D. W. 2014. Increasing muscle mass improves vascular function in obese (db/db) mice. *J. Am. Heart Assoc.* **3**: e000854. [Medline] [CrossRef]
27. Rodríguez, A., Becerril, S., Ezquerro, S., Méndez-Giménez, L. and Frühbeck, G. 2017. Crosstalk between adipokines and myokines in fat browning. *Acta Physiol. (Oxf.)* **219**: 362–381. [Medline] [CrossRef]
28. Sahu, A. 2004. Minireview: A hypothalamic role in energy balance with special emphasis on leptin. *Endocrinology* **145**: 2613–2620. [Medline] [CrossRef]
29. Schönke, M., Björnholm, M., Chibalin, A. V., Zierath, J. R. and Deshmukh, A. S. 2018. Proteomics analysis of skeletal muscle from leptin-deficient ob/ob mice reveals adaptive remodeling of metabolic characteristics and fiber type composition. *Proteomics* **18**: e1700375. [Medline] [CrossRef]
30. Turpin, S. M., Ryall, J. G., Southgate, R., Darby, I., Hevener, A. L., Febbraio, M. A., Kemp, B. E., Lynch, G. S. and Watt, M. J. 2009. Examination of 'lipotoxicity' in skeletal muscle of high-fat fed and ob/ob mice. *J. Physiol.* **587**: 1593–1605. [Medline] [CrossRef]
31. Wakayama, Y. 1976. Electron microscopic study on the satellite cell in the muscle of Duchenne muscular dystrophy. *J. Neuropathol. Exp. Neurol.* **35**: 532–540. [Medline] [CrossRef]
32. Wakayama, Y., Hirako, S., Jimi, T. and Shioda, S. 2015. AQP7 Up-regulation in the skeletal muscles of mice with diet induced obesity. *J. Cell Sci. Ther.* **6**: 2. [CrossRef]
33. Wakayama, Y., Hirako, S., Ogawa, T., Jimi, T. and Shioda, S. 2014. Upregulated expression of AQP 7 in the skeletal muscles of obese ob/ob mice. *Acta Histochem. Cytochem.* **47**: 27–33. [Medline] [CrossRef]
34. Wakayama, Y., Inoue, M., Kojima, H., Jimi, T., Shibuya, S., Hara, H. and Oniki, H. 2004. Expression and localization of aquaporin 7 in normal skeletal myofiber. *Cell Tissue Res.* **316**: 123–129. [Medline] [CrossRef]
35. Wakayama, Y., Jimi, T., Inoue, M., Kojima, H., Murahashi, M., Kumagai, T., Yamashita, S., Hara, H. and Shibuya, S. 2002. Reduced aquaporin 4 expression in the muscle plasma membrane of patients with Duchenne muscular dystrophy. *Arch. Neurol.* **59**: 431–437. [Medline] [CrossRef]
36. Wakayama, Y., Schotland, D. L., Bonilla, E. and Orecchio, E. 1979. Quantitative ultrastructural study of muscle satellite cells in Duchenne dystrophy. *Neurology* **29**: 401–407. [Medline] [CrossRef]
37. Wang, X., Hu, Z., Hu, J., Du, J. and Mitch, W. E. 2006. Insulin resistance accelerates muscle protein degradation: Activation of the ubiquitin-proteasome pathway by defects in muscle cell signaling. *Endocrinology* **147**: 4160–4168. [Medline] [CrossRef]
38. Warmington, S. A., Tolan, R. and McBennett, S. 2000. Functional and histological characteristics of skeletal muscle and the effects of leptin in the genetically obese (ob/ob) mouse. *Int. J. Obes. Relat. Metab. Disord.* **24**: 1040–1050. [Medline] [CrossRef]
39. Wein, S., Ukropec, J., Gasperíková, D., Klimes, I. and Seböková, E. 2007. Concerted action of leptin in regulation of fatty acid oxidation in skeletal muscle and liver. *Exp. Clin. Endocrinol. Diabetes* **115**: 244–251. [Medline] [CrossRef]
40. Xu, P., Werner, J. U., Milerski, S., Hamp, C. M., Kuzenko, T., Jähnert, M., Gottmann, P., de Roy, L., Warnecke, D., Abaei, A., Palmer, A., Huber-Lang, M., Dürselen, L., Rasche, V., Schürmann, A., Wabitsch, M. and Knippschild, U. 2018. Diet-induced obesity affects muscle regeneration after murine blunt muscle trauma-a broad spectrum analysis. *Front. Physiol.* **9**: 674. [Medline] [CrossRef]
41. Zhou, Y., Tan, Y., Hou, G., Ren, Y., Deng, Y., Yan, K., Zhang, Y., Lin, L., Lou, X. and Liu, S. 2020. Pathway attenuation of fatty acid beta-oxidation in the skeletal muscle of a type 2 diabetic mouse model. *Rapid Commun. Mass Spectrom.* **34**: e8869. [Medline] [CrossRef]